Brief Communications

A New Code for Contrast in the Primate Visual Pathway

Chris Tailby,[1] Samuel G. Solomon,[2] Neel T. Dhruv,[1] Najib J. Majaj,[1] Sach H. Sokol,[1] and Peter Lennie[1]

[1]Center for Neural Science, New York University, New York, New York 10003, and [2]Bosch Institute and School of Medical Sciences, The University of Sydney, New South Wales 2006, Australia

We characterize a hitherto undocumented type of neuron present in the regions bordering the principal layers of the macaque lateral geniculate nucleus. Neurons of this type were distinguished by a high and unusually regular maintained discharge that was suppressed by spatiotemporal modulation of luminance or chromaticity within the receptive field. The response to any effective stimulus was a reduction in discharge, reminiscent of the "suppressed-by-contrast" cells of the cat retina. To a counterphase-modulated grating, the response was a phase-insensitive suppression modulated at twice the stimulus frequency, implying a receptive field comprised of multiple mechanisms that generate rectifying responses. This distinctive nonlinearity makes the neurons well suited to computing a measure of contrast energy; such a signal might be important in regulating sensitivity early in visual cortex.

Key words: **vision; macaque; lateral geniculate; LGN; retina; receptive field; nonlinear**

Introduction

The principal projections from the primate retina to the dorsal lateral geniculate nucleus (LGN) originate in the midget and parasol ganglion cells, and terminate in the parvocellular (P) and magnocellular (M) cells, respectively. Together, these streams comprise ~90% of all of the relay neurons found in the LGN (Perry et al., 1984; Lee, 1996; Solomon, 2002; Wassle, 2004). P and M cells have center-surround receptive fields in which spatial summation is generally well described by linear models (Kaplan et al., 1990; Lee, 1996).

Midget and parasol ganglion cells are two of the ~15–20 morphological classes of ganglion cells in the primate retina. Other classes also project to the LGN (Dacey et al., 2003; Wassle, 2004), among them neurons that draw substantial input from short-wavelength-sensitive (S) cones, and whose signal summation within receptive fields is also generally well described by linear models (Derrington et al., 1984; Dacey and Lee, 1994; Martin et al., 1997; Dacey et al., 2003). Neurons with patently nonlinear receptive fields also exist (Schiller and Malpeli, 1977; Casagrande, 1994; White et al., 2001), but they have not been characterized, and are not accommodated in models of visual perception.

Here, we characterize a distinctive and homogeneous class of neuron in the macaque LGN. This has a regular and rapid spontaneous discharge that is suppressed by spatiotemporal contrast presented at any location within the receptive field. They resemble the "suppressed-by-contrast" neurons found in the cat retina and LGN (Rodieck, 1967; Stone and Hoffmann, 1972; Cleland and Levick, 1974).

Received Dec. 11, 2006; revised March 13, 2007; accepted March 14, 2007.

This work was supported by National Institutes of Health Grants EY04440 and EY13079, and Australian National Health and Medical Research Council Grant 211247 to S.G.S. We thank J.A. Movshon and W. Levick for helpful discussions.

Correspondence should be addressed to Chris Tailby at the above address. E-mail: ctailby@unimelb.edu.au.

DOI:10.1523/JNEUROSCI.5343-06.2007

 0270-6474/07/273904-06$15.00/0

Materials and Methods

Extracellular single-unit recordings were made from LGNs of eight anesthetized, paralyzed juvenile male *Macaca fasicularis*. The preparation and recording were as described previously (Solomon and Lennie, 2005). The microelectrodes were tungsten-in-glass (Merrill and Ainsworth, 1972). All procedures conformed to the guidelines approved by the New York University Animal Welfare Committee. Stimuli were presented on a calibrated cathode ray tube monitor (Vision Master Pro 514; Iiyama, Nagano, Japan) refreshed at 200 Hz and viewed from 114 cm, at which distance the screen subtended 15° × 20°. For some neurons, we also measured responses at lower refresh rates. Stimuli were defined by spatiotemporal modulations of luminance or chromaticity about a white point (Commission Internationale de l'Eclairage coordinates, $x = \sim 0.30$, $y = 0.32$) at a mean luminance of ~33 cd/m^{-2}. The stimulus was an 8°-diameter patch containing a drifting sinusoidal grating or a temporally modulated spatially uniform field. The rest of the screen was held at the mean luminance. Unless otherwise stated, the stimulus was achromatic and of full contrast. From the impulses discharged by each cell, we extracted the mean rate and the amplitude of the Fourier component at the frequency of stimulation (and in some cases the amplitude at twice that frequency). To characterize the tuning curves, we fit models of the form $R_{pred} = \lfloor MD - F(x) \rfloor^+$, where R_{pred} is the predicted mean discharge in the presence of the stimulus, MD is the maintained discharge to the mean luminance, $F(x)$ is a function describing tuning along the stimulus dimension of interest, and the operation $\lfloor \rfloor^+$ sets negative responses to 0 (rectification). We derived model fits by minimizing the χ^2 error between the model predictions and the observed discharge rate in Matlab (version 7.0; Mathworks, Natick, MA).

Results

The 12 neurons whose receptive fields are described here were encountered during a larger series of experiments on LGN. The first five neurons were fortuitously discovered in one monkey, and in subsequent experiments on seven animals we directed electrode penetrations to maximize the chance of encounter. We found seven more neurons in four of the monkeys. Throughout we will refer to these neurons as "suppressed-by-contrast" cells, because in many respects their receptive fields resemble those of the cat retinal ganglion cells described by Rodieck (1967).

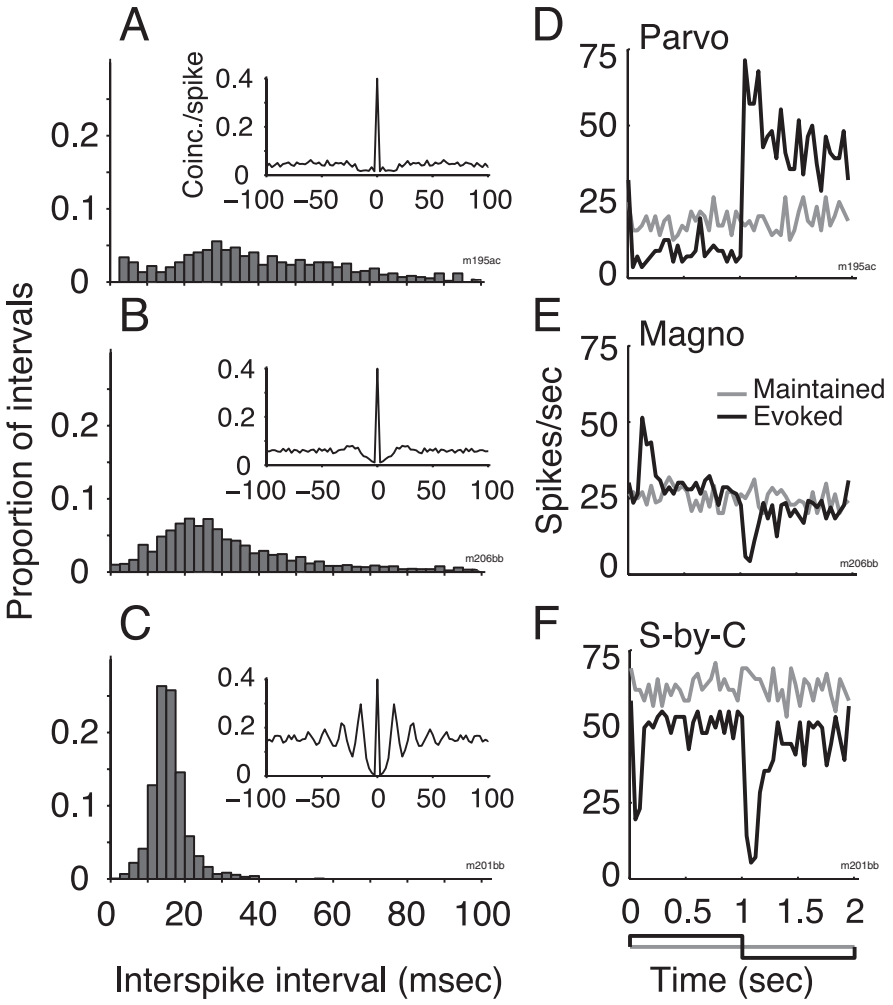

Figure 1. A class of cell in the primate LGN that is suppressed-by-contrast. ***A–C***, Interspike interval histograms and autocorrelation functions (sampled at 1 ms resolution) for the maintained discharge of an off-center P cell (***A***), an on-center M cell (***B***) and a suppressed-by-contrast neuron (***C***). ***D–F***, The responses of the same cells to full contrast square-wave temporal modulation of a large disc. Black lines, Averaged responses (in bins of 40 ms) during stimulation; gray lines, maintained discharge. The temporal profile of the stimulus is shown at the bottom.

Identification

The maintained discharge of suppressed-by-contrast cells was distinctively high, averaging 45.4 spikes/s (SD, 12.7; $n = 12$) when the animal viewed a uniform gray screen refreshed at 200 Hz. Under the same viewing conditions, the average maintained discharge of P-cells was 15.9 spikes/s (SD, 10.9; $n = 250$), of blue-yellow opponent cells, 20.0 spikes/s (SD, 12.2; $n = 87$), and of M-cells, 15.1 spikes/s (SD, 9.9; $n = 113$) (Troy and Lee, 1994). The interspike interval histograms and autocorrelograms in Figure 1*A–C* make clear that the maintained discharge of suppressed-by-contrast cells is also much more regular than that of P and M cells measured under the same conditions. This regularity can be characterized by the coefficient of variation (CV: the SD of the interval distribution divided by its mean; for a random spike train, the CV is 1 and for a regular spike train the CV is 0). In suppressed-by-contrast cells, the average CV was 0.61 (SD, 0.23), significantly lower than the corresponding CV values for P cells ($\mu = 0.87$; SD, 0.27; $n = 193$), M cells ($\mu = 0.86$; SD, 0.17; $n = 64$), and blue-yellow opponent cells ($\mu = 0.95$; SD, 0.40; $n = 80$) (Troy and Lee, 1994). The regularity of the discharge of suppressed-by-contrast cells was unrelated to the monitor refresh rate (200 Hz): the modal interspike interval for the cell shown in Figure 1*C* is 16.6 ms; across all cells, the modal interval ranged from 13.6 to 22.9 ms (median, 15.4; SD, 2.8).

In every suppressed-by-contrast cell, the spontaneous discharge was reduced by the presence of spatiotemporal contrast within the receptive field, regardless of the polarity of that contrast. Figure 1*F* shows for one cell the pattern of discharge during square-wave luminance modulation of a large disc centered on its receptive field. Transient reductions in discharge occurred at both the on and off phases of the modulation. This behavior is fundamentally different from that of M and P cells: the discharge of an on-center P or M cell (Fig. 1*E*) increases in response to a luminance increment and decreases in response to a luminance decrement (*vice versa* for an off-center cell) (Fig. 1*D*). We found no stimulus that increased the discharge of a suppressed-by-contrast cell above the maintained rate (see Discussion).

Anatomical location

All suppressed-by-contrast cells had monocular receptive fields: three had receptive fields in the contralateral eye and were encountered in the region separating the two most ventral P layers, and the remaining nine had receptive fields in the ipsilateral eye and were encountered in the region separating the most ventral P layer and the dorsal M layer. We did not make lesions at the recording sites to preserve the electrodes, but the locations were unambiguous given the pattern of transitions between eye representations, the low background activity at the transitions, and the functional properties of the cells on either side of these transitions. The receptive fields of the suppressed-by-contrast cells were located at eccentricities between 2 and 15° in the contralateral hemifield in positions consistent with those of M and P cells found near them.

Spatial frequency tuning

The spatial frequency tuning curves of suppressed-by-contrast cells were weakly bandpass and very similar from cell to cell (Fig. 2*A*, individual cell, *B*, average across the 10 cells for which we obtained these measurements). At mid to high spatial frequencies, the mean rate of discharge was suppressed uniformly throughout the drift cycle; there was no modulated component of the discharge of the kind that characterizes P and M cells. Very low spatial frequencies (including modulation of a spatially uniform field) reduced the mean discharge while also modulating the discharge at the stimulus frequency. The modulated response to a uniform field resembled half-wave rectification of the input signal: discharge was suppressed completely during the off phase of the modulation and less, if at all, during the on phase. At no point in the cycle did the discharge exceed the spontaneous rate (Fig. 2*A*, PSTH, inset). No suppressed-by-contrast cells were orientation selective. In what follows, we use the reduction in mean

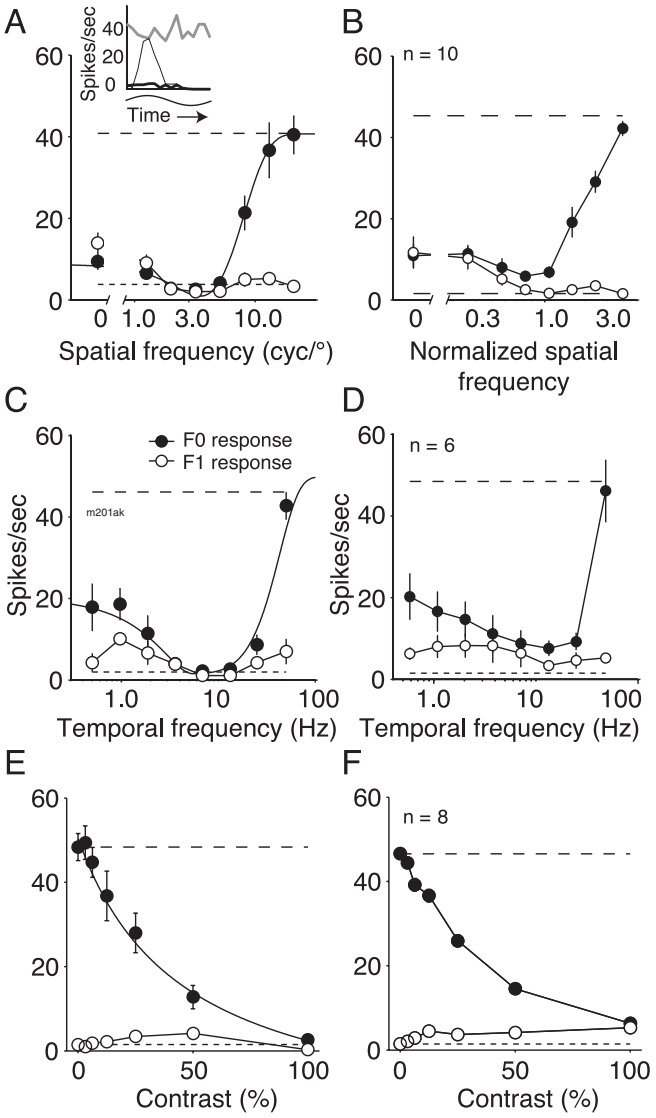

Figure 2. Spatiotemporal tuning and contrast sensitivity of suppressed-by-contrast cells. ***A***, ***B***, Spatial frequency tuning of a representative cell (temporal frequency, 5 Hz; ***A***) and the average curve for all cells (***B***; spatial frequency is normalized to the frequency of maximum suppression, on average 1.9 cycles/deg). Filled circles, Average discharge rate during presentation of a grating; open circles, amplitude of the modulated response at the frequency of stimulation (F1). Error bars show ±1 SEM. Dashed lines show the average rate of spontaneous discharge (top line) and the average spontaneous F1 (bottom line). Inset shows maintained discharge (gray line) and average response to passage of one cycle of the grating at each of two spatial frequencies (thin black line, 0 cycles/deg; thick black line, 8 cycles/deg). ***C***, ***D***, Temporal frequency tuning of the same cell as in ***A*** (spatial frequency, 3 cycles/deg; ***C***) and the average curve for all cells (***D***), obtained using drifting gratings of the most suppressive spatial frequency. ***E***, ***F***, Response as a function of contrast for the same cell as in ***A***, ***C*** (spatial frequency, 3 cycles/deg; temporal frequency, 9 Hz; ***E***) and averaged over all cells (***F***). Other conventions are as in ***A***.

discharge rate to measure the stimulus selectivity of the suppressive mechanism.

To characterize the spatial frequency tuning, we fit the suppression with a difference of Gaussians model (D-o-G) (Enroth-Cugell and Robson, 1966). The most suppressive spatial frequency was 1.9 cycles/deg (geometric mean, $n = 10$), similar to the optimum spatial frequency for modulation of P cells and exceeding that of M cells. These relationships are reflected in the center sizes returned by the D-o-G model: for suppressed-by-contrast cells, the geometric mean center radius was 0.064° (SD, 0.03), and for P cells and M cells at comparable eccentricities, 0.067° (SD, 0.05; $n = 170$) and 0.094 deg (SD, 0.04; $n = 61$).

Temporal frequency tuning

Suppressed-by-contrast cells had bandpass temporal frequency tuning curves (Fig. 2*C*, individual cell, *D*, average of six cells). To characterize temporal tuning, we used a descriptive function (Webb et al., 2005). Across all cells, suppression was strongest at 14.6 Hz (geometric mean, $n = 6$). No cell was suppressed by counterphase modulation at 100 Hz (data not shown). Gratings drifting at low temporal frequency (0.5 Hz) were less effective, with the reduction in discharge being 69% of the maximum suppression observed. The temporal tuning lay between that of P and M cells: P cells preferred 12.4 Hz, and the response at the lowest frequency was 46% as effective as at the best ($n = 251$); M cells preferred 25.0 Hz, and the response at the lowest frequency was 25% as effective as at the best ($n = 110$) (Derrington and Lennie, 1984).

We measured the latency of suppression after presentation of a stimulus, and the latency of the increase in discharge after removal of a stimulus (Muller et al., 2003). The mean latency of suppression was 39.0 ms (SD, 3.8; $n = 11$) and the mean latency of increased discharge was 51.2 ms (SD, 12.9). For comparison, the latency of a comparably strong increment step response in on-center P cells was 40.5 ms (SD, 8.8; $n = 27$), and in on-center M cells was 31.9 ms (SD, 6.4; $n = 21$).

Contrast gain

Figures 2, *E* and *F*, shows how the mean discharge rate declined with increasing contrast of drifting gratings of the most effective spatial frequency (Fig. 2*E*, individual cell, *F*, average of eight cells). Over most of the range, the mean rate was inversely related to contrast. We fit a Naka-Rushton function to the data to determine the average contrast gain (the slope of the initial part of the contrast response function), which was −1.8 impulses/s/[% contrast]. This is higher than the average contrast gain of P cells (1.1), but substantially lower than that of M cells (5.9) (Kaplan and Shapley, 1986; Croner and Kaplan, 1995; Levitt et al., 2001).

Spatial summation

Drifting gratings suppressed the discharge of a suppressed-by-contrast cell but did not usually modulate it, suggesting that the underlying mechanism is insensitive to the spatial phase of the stimulus. We confirmed this in seven cells by measuring discharge to counterphase-modulated gratings of the most suppressive spatial and temporal frequencies. Figure 3*A* shows the results for one cell. At all spatial phases, the mean rate of discharge was reduced, with little modulation at the frequency of stimulation (F1) and substantial modulation at twice that frequency (F2). There was no "null" phase at which the discharge was unaffected by the stimulus. We used an index devised by Hochstein and Shapley (1976a) (the average of the F2 across spatial phases divided by the maximum F1 at any phase) to quantify the nonlinearity of spatial summation. The geometric mean index was 1.7 ($n = 7$), much greater than that for P or M cells (average 0.42 and 0.63, respectively) (Levitt et al., 2001). The phase-insensitive rectified responses to counterphase-modulated gratings, coupled with the high spatial resolution (Fig. 2), implies that the receptive field of the suppressed-by-contrast cell is comprised of an array of relatively small rectifying spatial subunits (Hochstein and Shapley, 1976b; Troy et al., 1989).

Receptive field size

The size of a linear receptive field characterized by the D-o-G model can be estimated from the spatial frequency tuning curve.

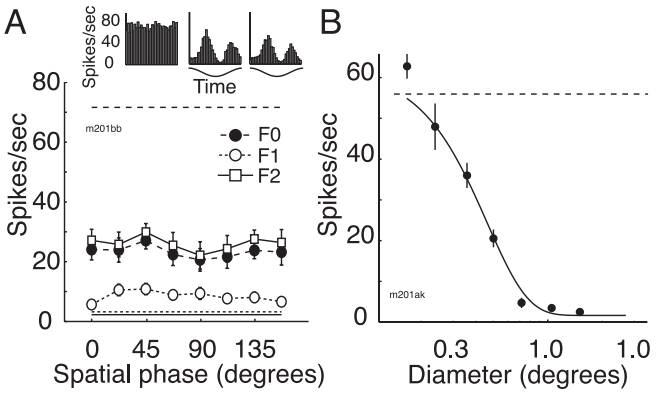

Figure 3. Spatial summation. ***A***, Average response of one suppressed-by-contrast cell to temporal modulation, as a function of the spatial phase of a counterphase-modulated grating of the preferred spatial (2.5 cycles/deg) and temporal frequency (6 Hz) and full contrast. Filled circles with dashed line, Mean rate of discharge; open circles with dotted line, amplitude of response at the frequency of stimulation (F1); open squares with solid line, amplitude of the response at twice the frequency of stimulation (F2). The amplitude of each of these components in the maintained discharge is shown by the horizontal lines of the corresponding style. Inset histograms show the average discharge in the absence of any stimulus (left) and during one cycle of modulation in two different spatial phases (center, 0°; right, 90°). Error bars show ±1 SEM. ***B***, Average discharge rate as a function of the size of a circular patch of grating (spatial frequency, 3 cycles/deg; temporal frequency, 9 Hz). Smooth curves show the fit of the model discussed in the text.

To estimate the size of the nonlinear receptive field of a suppressed-by-contrast cell, we obtained a size-tuning curve using patches of drifting grating of the most suppressive spatial and temporal frequencies. The set of responses was fit with the integral of a two-dimensional Gaussian (Fig. 3*B*), the characteristic radius of which was used as the measure of receptive field size. The geometric mean radius was 0.143° (SD, 0.083; $n = 7$). The geometric mean subunit size, inferred from spatial frequency measurements in the same cells was 0.055° (SD, 0.024). These measurements of receptive field size may be underestimates, because they were made with high-contrast stimuli, and the discharge was sometimes driven to zero for larger stimulus diameters.

Cone inputs

The receptive fields of some retinal ganglion cells have distinctive chromatic signatures: P (midget) cells compare the signals of long-wavelength-sensitive (L) and middle-wavelength-sensitive (M) cones; the small-bistratified cell receives strong excitatory input from S cones (Dacey and Lee, 1994). To characterize the chromatic signatures of suppressed-by-contrast cells, we measured responses to gratings modulated in different color directions about a white point (Derrington et al., 1984). In all 10 cells on which measurements were made, responses were suppressed strongly by isoluminant L–M modulation and by achromatic modulation, but only weakly by S-cone modulation. The signs and weights of cone inputs were estimated from a model that assumes a weighted sum of the signals of L, M, and S cones is full-wave rectified and subtracted from the maintained discharge (Lennie et al., 1990). We also explored a model in which cone signals were rectified before rather than after summation; this proved inadequate. The normalized weights of L- and M-cone inputs to the receptive fields of suppressed-by-contrast cells were on average 0.37 and −0.58, respectively (the signs are opposite, with that of the L cone arbitrarily positive), and for S cones the unsigned weight was 0.03. Suppressed-by-contrast cells are therefore substantially driven by opposed signals from L and M cones.

Discussion

We have characterized a distinctive and homogeneous class of cell not encountered previously in the LGN of macaque. We saw S potentials associated with the spikes recorded from three of our neurons and, although these were not well enough isolated to characterize the ganglion cell receptive fields, we think it likely that the distinctive receptive field properties are determined in the retina; De Monasterio and Gouras (1975), Schiller and Malpeli (1977), and de Monasterio (1978) have described primate ganglion cells whose discharge appeared to be suppressed by any visual stimulus.

The receptive fields of the cells we encountered resemble those of some rarely encountered retinal ganglion cells in cat [the suppressed-by-contrast cells (Rodieck, 1967; Stone and Hoffmann, 1972; Troy et al., 1989; Rowe and Cox, 1993); the uniformity detectors (Cleland and Levick, 1974)] and in rabbit (Levick, 1967; Amthor et al., 1989). Stone and Hoffmann (1972) observed that after removal of spatiotemporal contrast, the discharge of a suppressed-by-contrast cell was often briefly elevated above the maintained rate. We also saw this, and found that extending the duration of exposure to the suppressive stimulus led to greater poststimulus discharge, suggesting that it reflects habituation of the suppressive mechanism.

A complementary pathway that is excited by the presence of spatiotemporal contrast and insensitive to spatial phase (the "impressed-by-contrast" or "on–off" retinal ganglion cells) is present in the retinas of cat (Cleland and Levick, 1974; Troy et al., 1989) and monkey (De Monasterio and Gouras, 1975; Schiller and Malpeli, 1977; White et al., 2001). We encountered two apparently similar neurons in the macaque LGNs, but have not studied them systematically.

Receptive field model

Troy et al. (1989) provided a receptive field model for suppressed-by-contrast cells in cat, based on an earlier model of the Y cell developed by Hochstein and Shapley (1976b). In this model, the rectified activity of an array of subunits is subtracted from a maintained discharge. The subunits of the model presumably reflect bipolar cells whose normally excitatory output is rectified, as in Y cells (Demb et al., 2001), and inverted, either through an amacrine cell or directly via an inverting synapse. This model offers a potentially promising account of the observations here: the subunits provide fine spatial resolution and their rectified outputs make the suppressed-by-contrast cell sensitive to spatial frequencies beyond that expected from the size of its receptive field. If the subunits have a center-surround receptive field organization and their centers are small enough, drawing input from only a few cones, they would be sensitive to chromatic modulation (as has been proposed for P cells) (Lennie et al., 1991). The temporary increase in discharge after a prolonged stimulus might reflect a slowly recovering hyperpolarization in the bipolar cells themselves (Manookin and Demb, 2006).

Temporal modulation of a uniform field produced responses that do not fit easily with this model. We saw suppression at both on and off phases of square wave modulation (Fig. 1*C*), but for sinusoidal modulation there was no temporal frequency that gave rise to modulation at twice the frequency. At low temporal frequencies, the discharge rate dropped only during the off-phase of stimulation (Fig. 2*A*) (Rowe and Cox, 1993); at higher frequencies, the discharge was much lower than the maintained rate

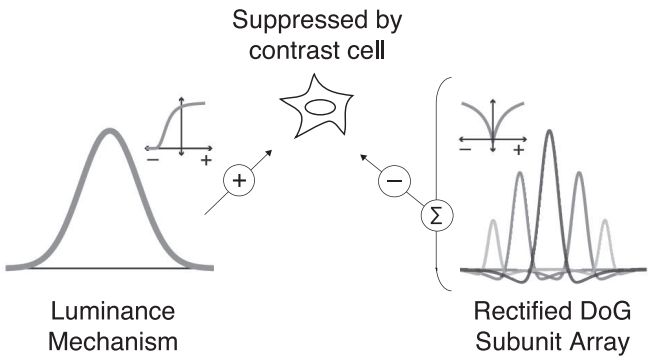

Figure 4. Model of receptive field. The discharge rate of suppressed-by-contrast cells reflects two sources of input: a spatially extensive light-driven source of excitation that controls the maintained discharge and has a Gaussian sensitivity profile (left), and a collection of rectifying, suppressive, subunits distributed over the receptive field (right). The spatial distribution of sensitivity within each subunit is represented by a difference of Gaussians.

throughout the cycle, and the modulation disappeared at rates of > 5 Hz (data not shown). The model above can produce the modulation at low temporal frequencies if the subunits are all off-center and their outputs are half-wave rectified (Demb et al., 2001) before subtraction from the maintained discharge, but this does not explain the responses at higher temporal frequencies, or the on–off suppression during square-wave modulation (Fig. 1). A small extension to the model, captured in Figure 4, might accommodate our results. We think that suppression arises in the rectified responses of a collection of on- and off-center subunits, all of which show strong spatial opponency and are thus largely ineffective at low spatial frequencies (the transient suppression for square wave modulation arising because the surround of the subunit slightly lags the center). Their summed output is subtracted from the maintained discharge, which is itself driven by a light-dependent excitatory mechanism that saturates. The discharge during sinusoidal modulation of a uniform field reflects the properties of this mechanism: the saturation prevents the discharge during modulation from ever exceeding the maintained rate and, at higher temporal frequencies, its effect is equivalent to a reduction in mean luminance (the mechanism is more sensitive to decrements than increments).

Rarity

Why have suppressed-by-contrast cells not been seen before in primate LGN? One reason may be that low monitor-refresh rates suppress the maintained discharge, from ~45 spikes/s at 200 Hz to ~20 spikes/s at 60 Hz (because the neurons respond to the frame updates). This removes the distinctiveness of the maintained discharge. Moreover, the usual practice of presenting contrast stimuli when searching for neurons while advancing the microelectrode will tend to silence a suppressed-by-contrast cell: brief decreases in discharge are harder to detect than brief increases. Finally, the location of these cells in the interlaminar regions suggests that they have small cell bodies that are consequently hard to record from (Rodieck, 1967; Cleland and Levick, 1974). Were the retinal coverage of suppressed-by-contrast cells the same as that of M cells, the relative densities of the two cell types could be estimated from their receptive field areas. Using our measurements of receptive field size of suppressed-by-contrast cells, and those of Croner and Kaplan (1995) for M cells, suppressed-by-contrast cells might be half the density of on-center (or off-center) M cells, and therefore probably no more than 2% of all ganglion cells.

Functional role

The retinogeniculate pathway is the main pathway by which information is transmitted from retina to visual cortex, and therefore the pathway most associated with visual awareness. The presence of suppressed-by-contrast cells in the LGN suggests that they might have some relatively direct access to visual sensation, although what their role might be is unclear. We would be better placed to understand this if we knew how suppressed-by-contrast cells behaved in natural visual environments: are they normally suppressed by the pattern of spatiotemporal contrasts imposed on their receptive fields by normal eye-movements, so that the absence of contrast (perhaps associated with a saccade) generates a discharge?

Cleland and Levick (1974) suggested a spike discharged by a suppressed-by-contrast cell indicates "no recent spatial or temporal discontinuities." Apart from the sign of its response, the suppressed-by-contrast cell differs from other known LGN cells in two notable ways: the regularity of its discharge and its indifference to stimulus phase. The regularity of discharge makes changes in firing rate potentially more detectable than would be the case if the maintained discharge resulted from a renewal process with the same mean rate and variability (Troy et al., 1989). The indifference to stimulus phase suggests that the cell can be thought of as computing a measure of contrast energy. Such a mechanism could be useful in setting contrast gain (Troy et al., 1989). This is an appealing possibility because it explains why it might be useful to have a highly nonlinear signal available as input to cortex.

References

Amthor FR, Takahashi ES, Oyster CW (1989) Morphologies of rabbit retinal ganglion cells with complex receptive fields. J Comp Neurol 280:97–121.

Casagrande VA (1994) A third parallel visual pathway to primate area V1. Trends Neurosci 17:305–310.

Cleland BG, Levick WR (1974) Properties of rarely encountered types of ganglion cells in the cat's retina and an overall classification. J Physiol (Lond) 240:457–492.

Croner LJ, Kaplan E (1995) Receptive fields of P and M ganglion cells across the primate retina. Vision Res 35:7–24.

Dacey DM, Lee BB (1994) The "blue-on" opponent pathway in primate retina originates from a distinct bistratified ganglion cell type. Nature 367:731–735.

Dacey DM, Peterson BB, Robinson FR, Gamlin PD (2003) Fireworks in the retina. Neuron 37:15–27.

Demb JB, Zaghloul K, Haarsma L, Sterling P (2001) Bipolar cells contribute to nonlinear spatial summation in the brisk-transient (Y) ganglion cell in mammalian retina. J Neurosci 21:7447–7454.

de Monasterio FM (1978) Properties of ganglion cells with atypical receptive-field organization in retina of macaques. J Neurophysiol 41:1435–1449.

De Monasterio FM, Gouras P (1975) Functional properties of ganglion cells of the rhesus monkey retina. J Physiol (Lond) 251:167–195.

Derrington AM, Lennie P (1984) Spatial and temporal contrast sensitivities of neurones in lateral geniculate nucleus of macaque. J Physiol (Lond) 357:219–240.

Derrington AM, Krauskopf J, Lennie P (1984) Chromatic mechanisms in lateral geniculate nucleus of macaque. J Physiol (Lond) 357:241–265.

Enroth-Cugell C, Robson JG (1966) The contrast sensitivity of retinal ganglion cells of the cat retina. J Physiol (Lond) 187:517–552.

Hochstein S, Shapley RM (1976a) Quantitative analysis of retinal ganglion cell classifications. J Physiol (Lond) 262:237–264.

Hochstein S, Shapley RM (1976b) Linear and nonlinear spatial subunits in Y cat retinal ganglion cells. J Physiol (Lond) 262:265–284.

Kaplan E, Shapley RM (1986) The primate retina contains two types of ganglion cells, with high and low contrast sensitivity. Proc Natl Acad Sci USA 83:2755–2757.

Kaplan E, Lee BB, Shapley R (1990) New views on primate retinal function. Prog Ret Res 9:273–336.

Lee BB (1996) Receptive field structure in the primate retina. Vision Res 36:631–644.

Lennie P, Krauskopf J, Sclar G (1990) Chromatic mechanisms in striate cortex of the macaque. J Neurosci 10:649–669.

Lennie P, Haake PW, Williams DR (1991) The design of chromatically opponent receptive fields. In: Computational models of visual processing (Landy MS, Movshon JA, eds), pp 71–82. Cambridge, MA: MIT.

Levick WR (1967) Receptive fields and trigger features of ganglion cells in the visual streak of the rabbits retina. J Physiol (Lond) 188:285–307.

Levitt JB, Schumer RA, Sherman SM, Spear PD, Movshon JA (2001) Visual response properties of neurons in the LGN of normally reared and visually deprived macaque monkeys. J Neurophysiol 85:2111–2129.

Manookin MB, Demb JB (2006) Presynaptic mechanism for slow contrast adaptation in mammalian retinal ganglion cells. Neuron 50:453–464.

Martin PR, White AJ, Goodchild AK, Wilder HD, Sefton AE (1997) Evidence that blue-on cells are part of the third geniculocortical pathway in primates. Eur J Neurosci 9:1536–1541.

Merrill EG, Ainsworth A (1972) Glass-coated platinum-plated tungsten microelectrodes. Med Biol Eng 10:662–672.

Muller JR, Metha AB, Krauskopf J, Lennie P (2003) Local signals from beyond the receptive fields of striate cortical neurons. J Neurophysiol 90:822–831.

Perry VH, Oehler R, Cowey A (1984) Retinal ganglion cells that project to the dorsal lateral geniculate nucleus in the macaque monkey. Neuroscience 12:1101–1123.

Rodieck RW (1967) Receptive fields in the cat retina: a new type. Science 157:90–92.

Rowe MH, Cox JF (1993) Spatial receptive-field structure of cat retinal W cells. Vis Neurosci 10:765–779.

Schiller PH, Malpeli JG (1977) Properties and tectal projections of monkey retinal ganglion cells. J Neurophysiol 40:428–445.

Solomon SG (2002) Striate cortex in dichromatic and trichromatic marmosets: neurochemical compartmentalization and geniculate input. J Comp Neurol 450:366–381.

Solomon SG, Lennie P (2005) Chromatic gain controls in visual cortical neurons. J Neurosci 25:4779–4792.

Stone J, Hoffmann KP (1972) Very slow-conducting ganglion cells in the cat's retina: a major, new functional type? Brain Res 43:610–616.

Troy JB, Lee BB (1994) Steady discharges of macaque retinal ganglion cells. Vis Neurosci 11:111–118.

Troy JB, Einstein G, Schuurmans RP, Robson JG, Enroth-Cugell C (1989) Responses to sinusoidal gratings of two types of very nonlinear retinal ganglion cells of cat. Vis Neurosci 3:213–223.

Wassle H (2004) Parallel processing in the mammalian retina. Nat Rev Neurosci 5:747–757.

Webb BS, Dhruv NT, Solomon SG, Tailby C, Lennie P (2005) Early and late mechanisms of surround suppression in striate cortex of macaque. J Neurosci 25:11666–11675.

White AJ, Solomon SG, Martin PR (2001) Spatial properties of koniocellular cells in the lateral geniculate nucleus of the marmoset *Callithrix jacchus*. J Physiol (Lond) 533:519–535.